

Report

R-18-10

December 2018



Detailed geomorphological analysis of LiDAR derived elevation data, Forsmark

Searching for indicatives of late- and postglacial seismic activity

Christian Öhrling

Gustaf Peterson

Henrik Mikko

SVENSK KÄRNBRÄNSLEHANTERING AB

SWEDISH NUCLEAR FUEL
AND WASTE MANAGEMENT CO

Box 3091, SE-169 03 Solna
Phone +46 8 459 84 00
skb.se

SVENSK KÄRNBRÄNSLEHANTERING

ISSN 1402-3091

SKB R-18-10

ID 1704689

December 2018

Detailed geomorphological analysis of LiDAR derived elevation data, Forsmark

Searching for indicatives of late- and postglacial seismic activity

Christian Öhrling, Gustaf Peterson, Henrik Mikko
Geological Survey of Sweden

Keywords: Postglacial faulting, Paleo-seismicity, LiDAR.

This report concerns a study which was conducted for Svensk Kärnbränslehantering AB (SKB). The conclusions and viewpoints presented in the report are those of the authors. SKB may draw modified conclusions, based on additional literature sources and/or expert opinions.

A pdf version of this document can be downloaded from www.skb.se.

© 2018 Svensk Kärnbränslehantering AB

Abstract

Here, we use LiDAR elevation data to screen the landscape for geomorphological indicators of glacially induced seismic activity, specifically late- to postglacial faulting (PGF). It is crucial for the planning of the spent nuclear fuel repository to survey the occurrence of PGF's, since the site for this purpose demand a geological environment that is stable over long-periods of time. The known faults of this type have always reused old weaknesses in the crust. To date, proved occurrences in Sweden are all located north of the study area, which cover 13 225 km², in central-eastern Sweden.

LiDAR-derived point cloud elevation data was used to compile a 1-meter resolution DEM, which provides good conditions to find traces of PGF's. The geomorphological criteria that we searched for were scarps that crosscut glacial deposits. Such scarps, found elsewhere, are commonly more than 1 km long and has a vertical displacement of several meters (c. 5–10 m).

We essentially confirmed previous assessments since no mapped landforms are clearly indicative of postglacial seismicity (i.e. glacial landforms displaced by faults) and have not unambiguously identified any glacially induced fault scarps or landslide scarps. However, two scarps require additional analyses by means of a field reconnaissance and excavation program to unambiguously determine if they are of a non- seismic origin, or not. None of these scarps are obvious or distinct in their appearance but cannot without further work be completely depreciated.

All of the screened area is situated below the highest marine limit, which mean that the landscape has been exposed to wave washing. This could have erased minor surficial traces of late- to post-glacial seismic activity.

Sammanfattning

Vi har använt LiDAR-höjddata till att manuellt kartera landskapet efter geomorfologiska indikatorer på sen- till postglacial seismisk aktivitet, specifikt förkastningar kopplade till glacialt inducerade rörelser i jordskorpan. För planeringen av slutförvaret av kärnbränsle är det av stort intresse att undersöka förekomsten av postglaciala förkastningar (PGF), eftersom förvaret kräver en stabil geologisk miljö under långa tidsrymder. Dokumenterade fall av PGF:ar har alltid återaktiverat en äldre svaghet i jordskorpan. Hitintills, har alla bevisade förekomster hittats längre norrut än vårt studieområde i centrala östra Sverige.

Punktmolnsdata från LiDAR-mätningar användes för att skapa en digital höjdmodell (DEM) med en upplösning av 1 meter. Denna höga rumsliga upplösning skapar goda förutsättningar att detektera spår efter PGF:ar i landskapet. En PGF bör enligt gängse definition kunna följas minst 1 km på ytan och ha en vertikal rubbning av flera meter (ca. 5–10 m).

Resultaten från studien har i stort bekräftat resultaten från tidigare studier och inga av de karterade landformerna visar tydliga tecken på postglacial seismisk aktivitet. Vi har alltså inte otvetydigt identifierat någon glacialt inducerad förkastningsbrant eller jordskredsbrant. Men, två branter bör undersökas närmre med ett fältrekognoserings- och utgrävningsprogram för att säkerställa huruvida de orsakats av postglacial seismicitet eller ej. Ingen av dessa branter är uppenbara eller distinkta, men kan inte helt uteslutas vara betingade av sen- till postglacial seismisk aktivitet utan ytterligare undersökningar.

Hela studieområdet ligger under den Högsta Kustlinjen (HK), vilket innebär att landskapet har varit utsatt för svallning och omlagring av vågor. Denna svallning kan ha suddat ut vissa spår av sen- till postglacial seismisk aktivitet.

Contents

1	Introduction	7
1.1	Purpose	7
1.2	Setting and background geology	7
1.3	Postglacial faults – definition and precursors	9
2	Methods and material	11
2.1	Spatial data	11
2.2	Screening procedure	11
3	Results and interpretations	13
3.1	Examples of scarps	13
4	Discussion	25
5	Conclusions	27
6	Suggested field-campaign program	29
7	Supplementary material	31
	References	33

1 Introduction

Post-glacial, or isostatic, rebound is the rise of the land mass associated with the retreat of the ice-sheet during the last glacial period, the Weichselian. The presence of the ice-sheet caused an isostatic depression in the order of up to 800 m along the northern Swedish Baltic coast. Most of this depression has been recovered with some tens of meters remaining (e.g. Lund et al. 2009 and references therein). Ice-sheet ice-sheet. The isostatic rebound has a vertical component, glacial isostatic uplift, and a horizontal component directed outward from the area of maximum depression which is increasing with the distance. Stress redistributions resulting from the advance and retreat of continental ice-sheets, combined with tectonic stresses, may under certain circumstances trigger seismic reactivation of faults (e.g. Lund and Näslund 2009, Muir-Wood 2000).

Detection of paleoseismicity requires the application of geologic, stratigraphic, geomorphic, structural and geophysical criteria (Fenton 1999, Lund and Näslund 2009). Here, we use a method based on geomorphology and screen the landscape for scarps with crosscutting relations that could indicate that there has been movement along the scarp after the glacial deposits were laid down (i.e. post-glacial).

1.1 Purpose

The purpose of this study is to investigate if seismic activity has affected a larger area around Forsmark since the final retreat of the Weichselian ice-sheet. Due to the availability of high resolution LiDAR (Light detection and ranging) elevation data, which reveal landscape details not seen before (see Johnson et al. 2015), SKB assigned the Swedish Geological Survey (SGU) the task with analysing this data for indicators of postglacial seismic activity. SGU has extensive experience with this kind of analyses and questions, both without LiDAR information (Lagerbäck and Henkel 1977, Lagerbäck and Sundh 2008, Lagerbäck et al. 2005, Lundqvist 2000, 2010) and with LiDAR derived elevation models (Mikko et al. 2015, Smith et al. 2014). This report concentrates on the mapping of postglacial fault (PGF) scarps and landslide scarps. The present work is thus complementary to the thorough investigations within the study area performed by Lagerbäck et al. (2005).

1.2 Setting and background geology

The screened area is 13 225 km² and cover parts of the provinces of Uppland and Gästrikland (Figure 1-1), whereof the main part is located in Uppland. Along the Baltic Sea coast, at the centre of the study area, lies the Forsmark nuclear plant and the Söderviken candidate area – the selected location for the spent fuel repository. The fuel is environmentally hazardous for at least 100 000 years (Hedin 1997, SKB 2011) and therefore requires a stable geological environment. The majority of the study area has a low bedrock relief, as the area constitute part of the sub-Cambrian peneplain (Lidmar-Bergström 1982), a mega-scale geomorphological erosional-unconformity feature. The bedrock belongs to the Svecokarelian orogen in the south-western parts of the Fennoscandian Shield and it generally consists of granitoids. Stephens et al. (2008) present a detailed description of the bedrock in the Söderviken area. The surficial deposits are in general thin (<0.5m) or discontinuous along the coast and in higher grounds. Relatively larger depths are found in the valleys (c. 5 m) with the thickest deposits in eskers (more than 50 m in the Uppsala esker) (Hedenström et al. 2008, SGU 2015a). There are two major eskers: Uppsala esker, which has feeding branches in the Vattholma, Västland and Husby eskers; and the Enköping (alternatively Heby or Hedesunda) esker that have a major contributory branch from the Färnebo esker. The fine-grained deposits in the coastal areas are often of a postglacial origin. Extensive erosion, due to strong coastal currents and low relief (cf. Hedenström and Risberg 2003, Persson 1988), remobilised the glacial clays. The Forsmark site (approx. 12 km²) is thoroughly described in Söderbäck (2008) and the surficial-deposit map (42 km²) is described in Sohlenius et al. (2004).

The last ice-sheet retreat over the area occurred approximately 11 000 years ago (Hughes et al. 2016, Pässe and Daniels 2015, Stroeven et al. 2016), leaving a glacially sculpted landscape below the Yoldia Sea surface – the entire study area is below the highest coastline (SGU 2015b). As a result of the glacial isostatic rebound, the land rose from the Yoldia sea and was exposed to the erosive forces of waves and strong currents, which redistributed sediments in the landscape. 31 percent of the area in Figure 1-1 is still below the Baltic Sea surface, however, that part lacks LiDAR data and is consequently not screened.



Figure 1-1. The study area in eastern Sweden, delimited by the blue rectangle. Forsmark nuclear powerplant and the Söderviken area are 15 km northwest of Östhammar.

1.3 Postglacial faults – definition and precursors

With remote sensing, a postglacial fault (PGF) can be detected as a geomorphic feature crosscutting surficial sediments or landforms (i.e. it does not align with deglacial patterns) deposited or formed during the last ice covered period. Thus, postglacial faulting is by definition occurring in recently deglaciated regions (Fenton 1999). According to Fenton (1999), a PGF is generally; a reverse-type fault, a kilometer or more in length, have higher displacement to length ratios than similar sized tectonic faults, and are often oriented normal to the maximum horizontal stress (Figure 1-2).

PGF's have historically been searched for on aerial photographs, where spatially extensive scarps in the terrain, with a fresh appearance, were mapped and field checked. This resulted in several mapped scarps in northern Sweden (Lagerbäck and Henkel 1977, Lagerbäck and Sundh 2008, Lundqvist and Lagerbäck 1976, Mörner 2005) and these are also the most prominent scarps when studying them in LiDAR derived elevation data. Thus, in recent years the availability of LiDAR have given researchers the opportunity to detect scarps not previously seen (Berglund and Dahlström 2015, Mikko et al. 2015, Palmu et al. 2015, Smith et al. 2014). Furthermore, Mikko et al. (2014) recently discovered a fault scarp in Bollnäs, the closest to Forsmark proven PGF – 48 km NNW of the study area (Smith et al. 2014).

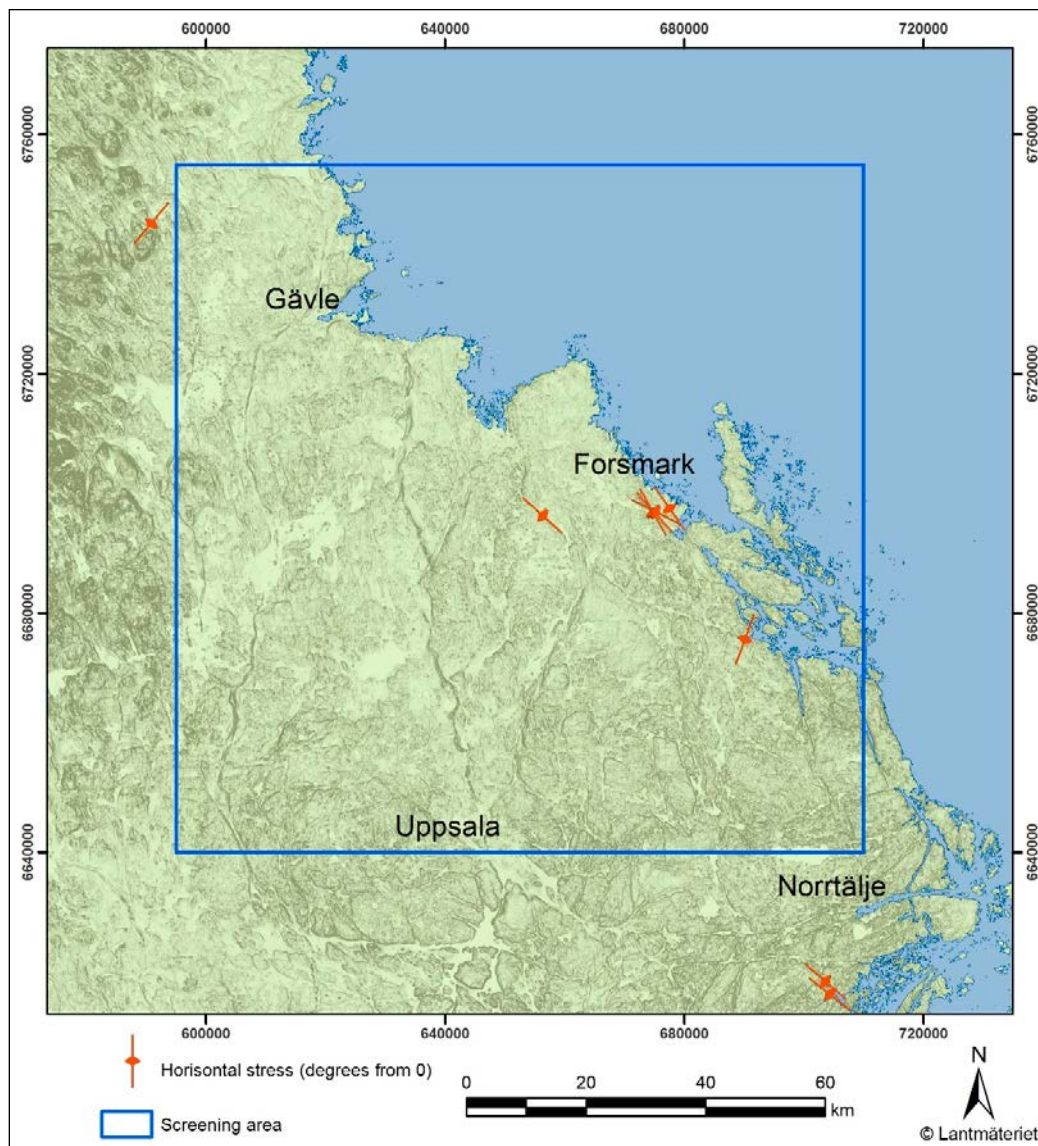


Figure 1-2. Map of the horizontal stress in the area. Lines are recorded measurements compiled in the World stress map (Heidbach et al. 2016), with one measure at Forsmark added here (Martin 2007). Background map show the slope function of the DEM.

2 Methods and material

Lineaments and scarps have been manually mapped using a digital drawing board – Wacom CINTIQ 27". Most mapping and analysis of data were performed using ESRI ArcGIS ArcMap 10.5, while a few data sets were produced with GRASS and QGIS.

2.1 Spatial data

The official LiDAR-based elevation data provided by Lantmäteriet have a horizontal resolution of 2 meters and is produced from a point cloud with elevation data retrieved from an airborne LiDAR sensor. The resolution of 2 meters is chosen based on the amount of measured points that can be automatically classified as ground. Within forested areas the amount of measured points classified as ground are less than in open areas due to scattering. Thus, in open areas, with little or no trees, it is possible to produce a DEM with a higher resolution (<2 m). The point cloud data set were used to produce a digital elevation model (DEM) with a cell-resolution of 1 meter. Consequently, this means that it is only in open areas where 1 meter resolution can be expected to be reasonable and without interpolation artefacts.

Additional background data used to interpret the landscape were also SGU's; Surficial Deposit Database, Drift Depth model, and geophysical data. Further, information from topographic maps (e.g. gravel pits or relics) and ortophotos were used.

2.2 Screening procedure

The geomorphological screening and analysis were conducted after the methods described by Mikko et al. (2015), with some additional analyses described in Table 2-1.

Hillshade maps were produced with a variation of illumination angles from 270°, 315°, 0°, 45° and 90° from north. Rasters with calculated slope, aspect and curvature analyses were also used. A filter (5° interval from 45° to 90°) on the slope model was used to highlight areas with a steep slope. These functions were all calculated with ESRI ArcGIS Tools. Moreover, GDAL tools (inside QGIS) was used to produce a topographical position index (TPI) model. Finally, two sets of geomorphon models – one based on 10 m resolution and one on 3 km – were modelled in GRASS GIS. Figure 2-1 displays ten different views – from the above-mentioned functions – of one example of lineament in the landscape.

Table 2-1: Short description of the GIS functions used for analyses.

ArcGIS function	Description of function
Hillshade	A grayscale 3D representation of the surface, with the sun's relative position considered for shading the image. This function uses the altitude and azimuth properties to specify the sun's position (ESRI 2018).
Slope	Slope represents the rate of change of elevation for each digital elevation model (DEM) cell. It is the first derivative of a DEM (ESRI 2018).
Aspect	Identifies the downslope direction of the maximum rate of change in value from each cell to its neighbours. Aspect can be thought of as the slope direction. The values of the output raster will be the compass direction of the aspect (ESRI 2018).
Curvature	Calculates the curvature of a raster surface, optionally including profile and plan curvature (ESRI 2018).
Topographic position index	Is defined as the difference between a central pixel and the mean of its surrounding cells (GDAL/OGR contributors, 2018). It provides an indication of whether any particular pixel forms part of a positive (e.g., crest) or negative (e.g., trough) feature of the surrounding terrain (Wilson et al. 2007).
Geomorphons	Geomorphons is a powerful way of quantitatively describe a landscape using mathematically predefined landscape elements (e.g. slope, ridge, valley, peak and more) (Jasiewicz and Stepinski 2013).

The approach to screen the assigned area was to first render a grid that was used to keep track of which areas were checked and which were not. Then each grid cell was screened for lineaments and scarps, starting with a zoom scale of approximately 1:15 000 and then zooming in on suspect lineaments (often in about 1:4 000). To get a better picture of the regional context it is sometimes needed to zoom out as well, to about 1:30–50 000. During this process, the background data was varied between the different datasets described above (Table 2-1 and Figure 2-1).

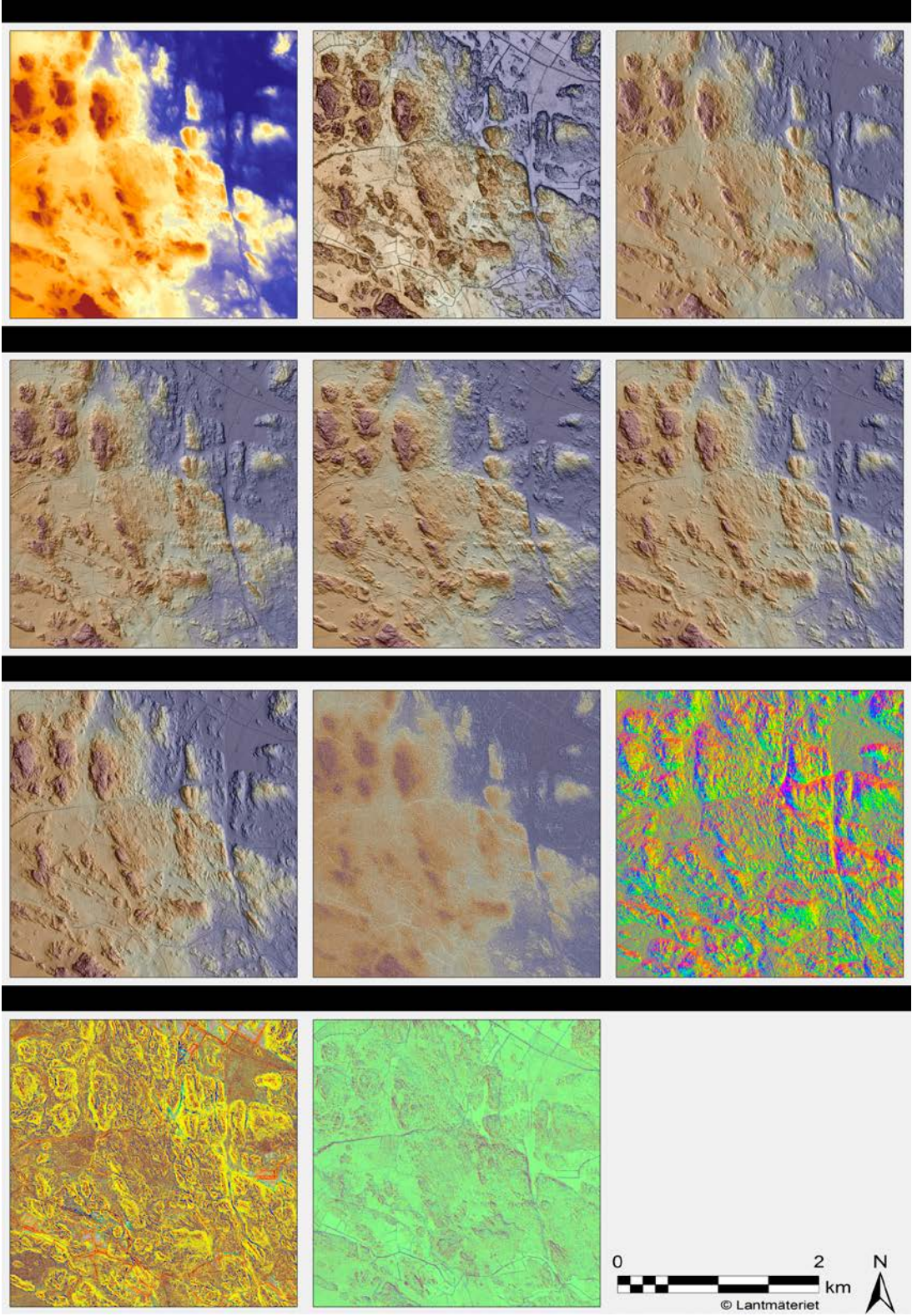


Figure 2-1. The derivatives, calculated from the LiDAR background data (DEM), used for interpretation.

3 Results and interpretations

Scarps seen in the LiDAR data have been mapped and in the following section examples of those are described and interpreted. An ESRI shape-file of mapped lineaments, including comments, is in the supplementary material, see section 7.

3.1 Examples of scarps

In total 66 scarps were mapped. Here we present a selection of the most interesting ones with figures – the location of these are displayed in Figure 3-1.

The most interesting scarp, in terms of morphological appearance, discovered here is shown in Figure 3-2. This scarp strikes parallel to a much larger lineation 1 km to the NE, which strengthens the PGF interpretation since they always reactivate old weaknesses in the crust (e.g. Lund and Näslund 2009). The scarp appears to cut several small ice-marginal moraines (De Geer moraines) and display a relatively fresh appearance – not seemingly affected by subsequent fluvial erosion. It can be followed for 1.5 km and has a vertical displacement of 3 m. This results in an aspect ratio of 0.002, which is high according to the criteria – Fenton (1999) call these “short, fat faults”.

Another scarp that appears to cut De Geer moraines is displayed in Figure 3-3. This example is not as convincing as Figure 3-2, since it is very short, and the offset cannot be convincingly determined. The lineation could be an erosional feature caused by subglacial meltwater. The moraine ridges would have formed at or close to the ice margin during deglaciation.

Murtoo is a recently discovered V-shaped subglacial landform (Figure 3-4) suggested to be produced during rapid retreat of the ice-sheet (Johnson et al. 2018). These can easily (but falsely) be interpreted as postglacial faults, especially when occurring as single features, as in Figure 3-4c, which is an interesting scarp – interpreted as a glaciofluvial erosional feature. A commonly occurring geomorphological feature in the study area are sharp eastward faced scarps that are closely related to murtoos. In a few places, such scarps delimit an apparent corridor (Figure 3-4d). These are glaciofluvial corridors (GFC's), thus a subglacially formed feature (e.g. Peterson and Johnson 2018, Utting et al. 2009).

Old bedrock lineaments are abundantly recognized in the LiDAR data. In Figure 3-5, an obvious lineament oriented NW-SE is displayed. It is not a PGF, but probably a weathered hypabyssal (i.e. intrusive igneous rock) rock. A less obvious scarp is also present, oriented WNW-ESE. It can be followed for 800 m and has a vertical offset of c. 1 m. This scarp cannot undoubtedly be dismissed from the list of potential PGF's.

An interesting scarp is displayed in Figure 3-6. It is slightly curved, can be followed 1 km and has an irregular offset. In the NE extension of the scarp line, a glaciofluvial scarp continues in the scarp direction. However, we propose that the scarp line and the glaciofluvial scarp are of different origin and only match by coincidence. We base this on the different appearances, the glaciofluvial part has a clear erosional scarp while the western part has not, and the observation of the continuation of glaciofluvial erosion southwards.

Figure 3-7 shows several scarps of which a W-E lineament in the centre is crossing a SSW-NNE scarp. The latter, is presumably younger and can be followed for 1.3 km and have a vertical displacement of 2 to 3 m. There is a large esker without any visible cut, 1.4 km in the SSW extension of the scarp (outside the figure). The inserted figure shows that there are indications of minor moraine ridges (dark blue arrows) crosscut by the scarp. In the upper part of the figure there is an moraine that seemingly superpose the lineament. If this scarp is a PGF, it would mean that the faulting event took place in the vicinity of the ice sheet margin.

The scarp in Figure 3-8 aligns with an end moraine in the eastward direction. It is interpreted as a bedrock-controlled scarp that has been enhanced by ice-marginal processes during deglaciation, for example by meltwater.

Figure 3-9 shows an old bedrock gorge, possibly shaped due to a weathered hypabyssal rock. Lineaments are also visible in the NNW-SSE orientation which appears to be a paleo ice-flow direction during the final retreat of the ice sheet (see Figure 3-11).

These kinds of analyses could perhaps be automated. However, it would probably be lots of work to clean out all falsely mapped scarps. Fig. 3-10 and 3-11 visualize a few examples of lineations and scarps that an automated mapping possibly would map. Figure 3-10 show several raised-beach ridges and modern fluvial scarps, while Figure 3-11 is full of glacial lineations oriented in the paleo ice-flow direction. An automated approach would in a landscape such as the study area (i.e. hilly bedrock relief and glacial landforms) map many scarps. However, it would be hard to discern the scarps based on genesis. We conclude that the manual approach is the most solid method for mapping fault scarps, the method is also well established and have been used in the region frequently (e.g. Lagerbäck and Henkel 1977, Lagerbäck and Sundh 2008, Lagerbäck et al. 2005, Lundqvist 2000, 2010, Mikko et al. 2015, Smith et al. 2014, Berglund and Dahlström 2015, Palmu et al. 2015). Nevertheless, the advancement in machine learning (and artificial intelligence) are fast and in the future, there might be other possibilities.

Landslides in the study area have been mapped previously (SGU 2016). None of these or any newly mapped landslide scarps, during the present study, are considered to be related to paleoseismicity.

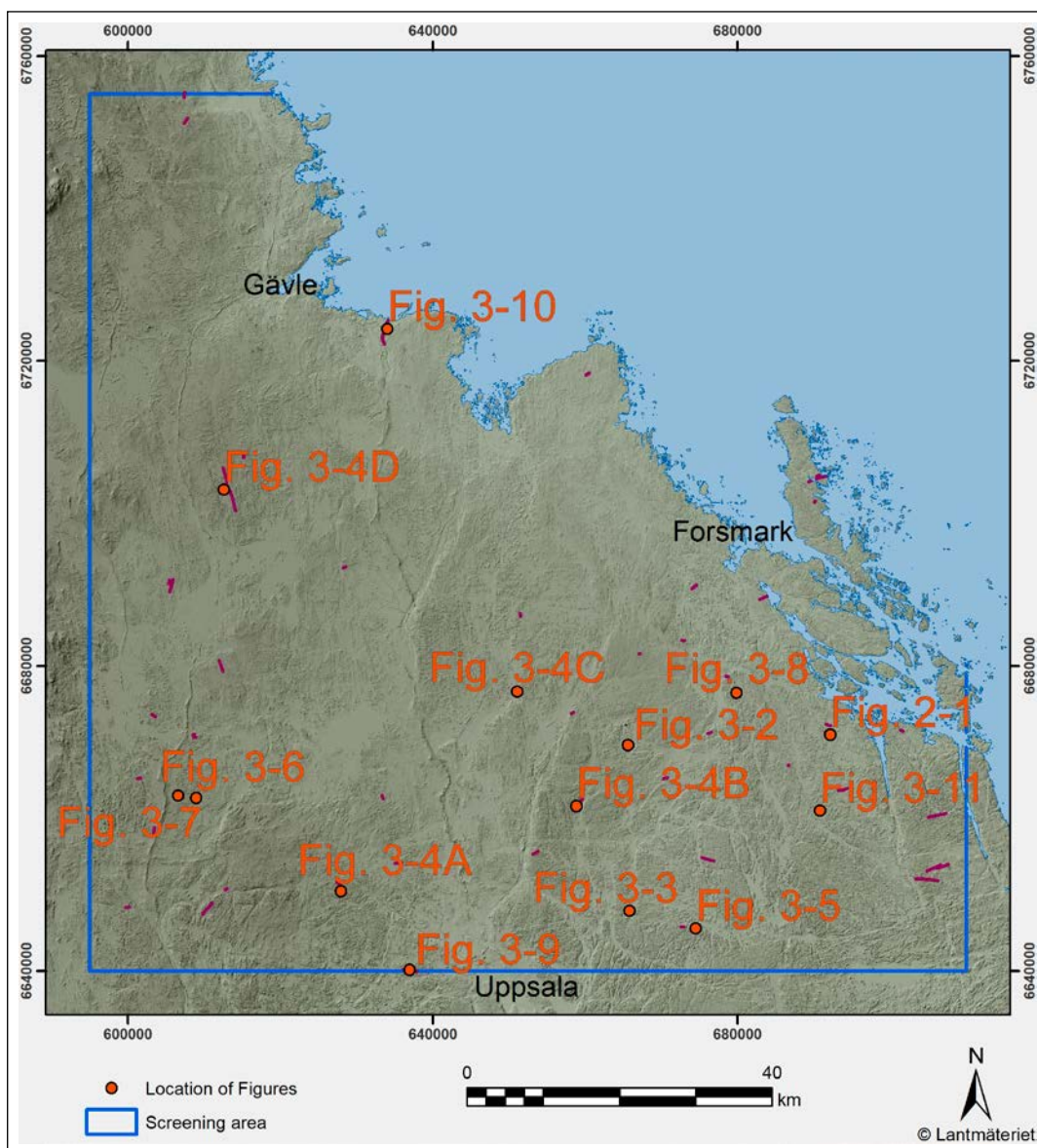


Figure 3-1. The locations of Figure 3-2 to 3-11 are displayed on a hillshade map of the study area.

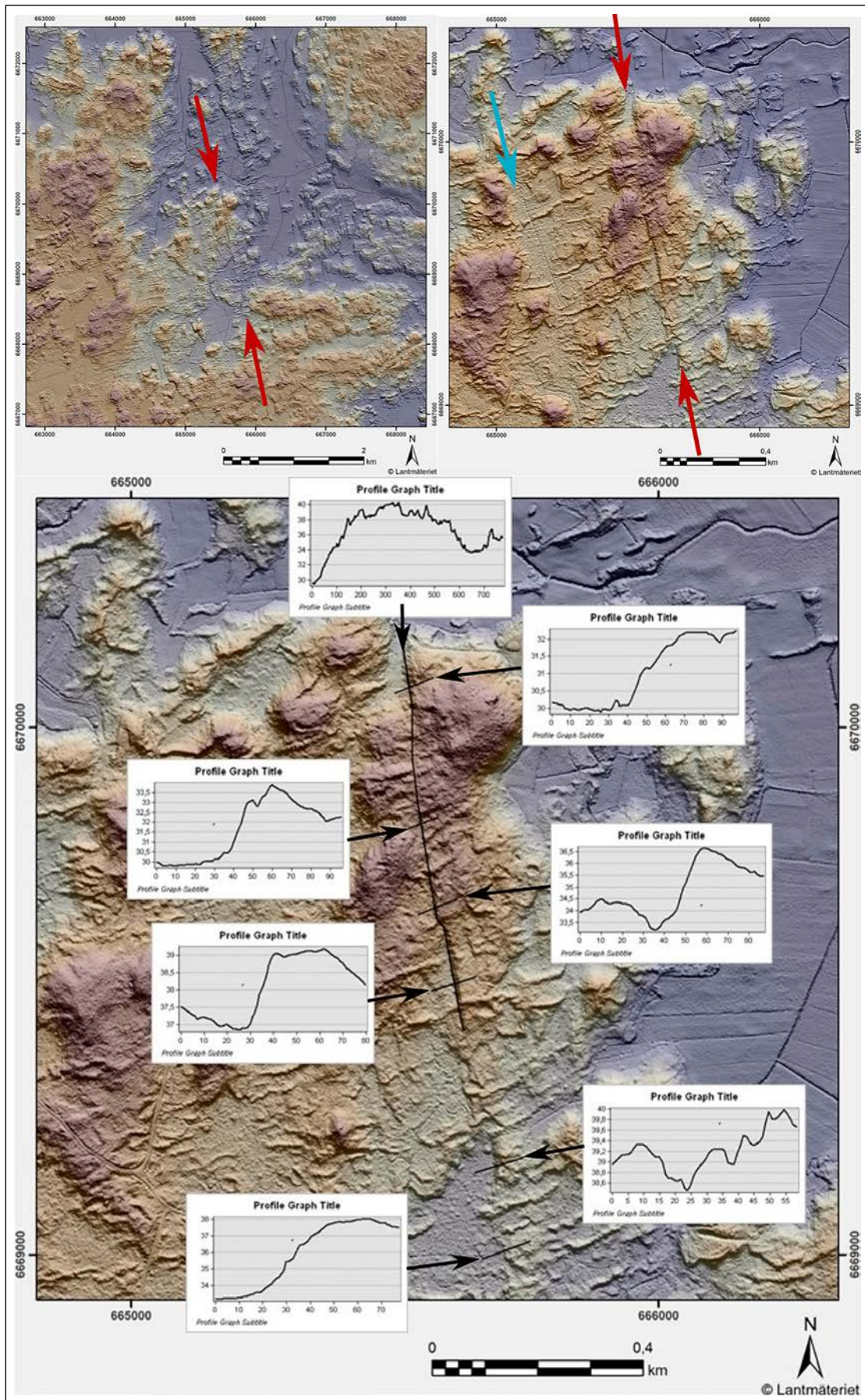


Figure 3-2. Scarp indicating a possible postglacial fault. Turquoise arrow show ice-flow direction and red arrows mark the scarp. Elevation profiles visualize the vertical offset along the scarp.

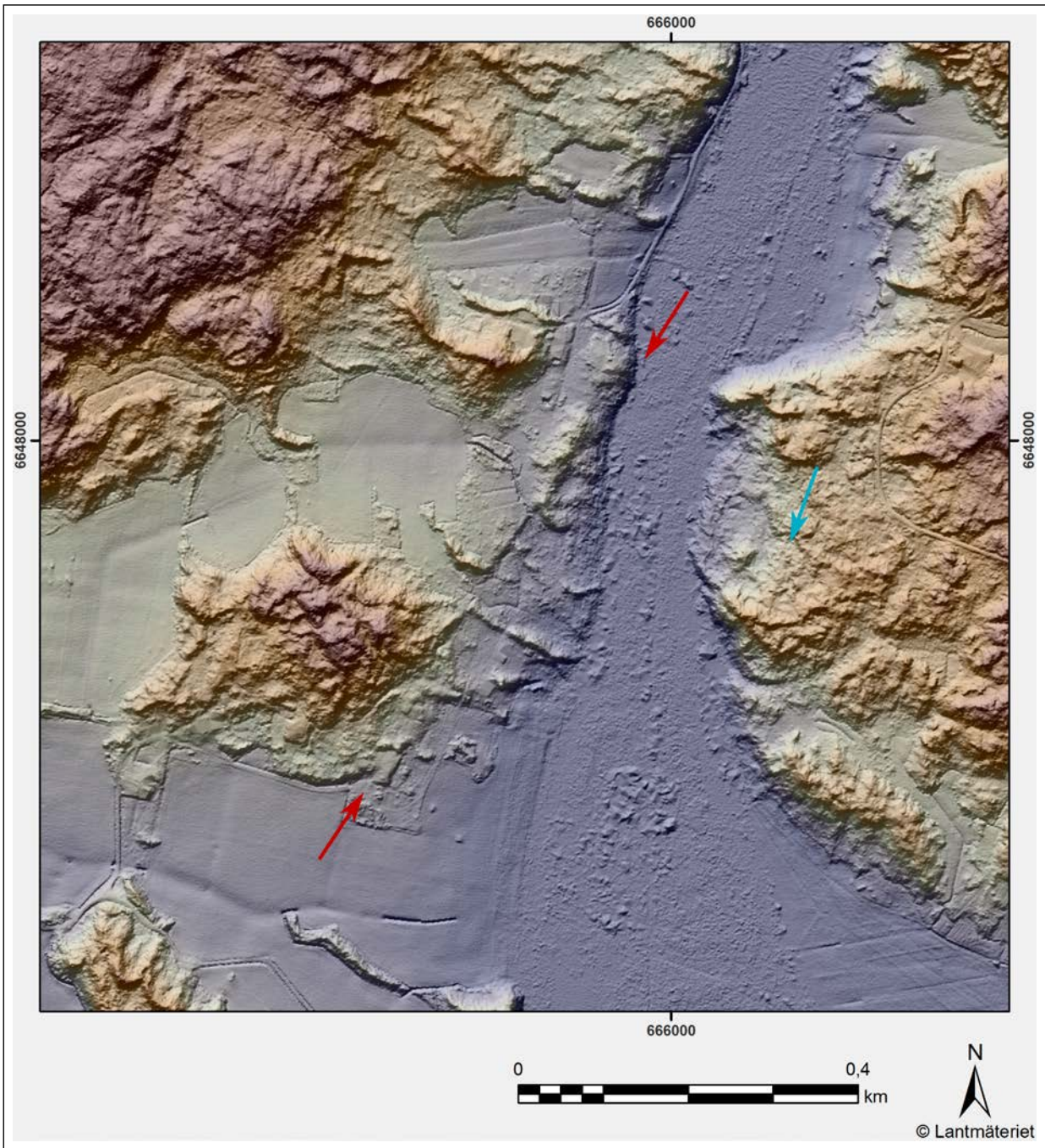


Figure 3-3. A scarp that appear to cut ice-marginal moraines. Turquoise arrow show ice-flow direction and red arrows mark the scarp.

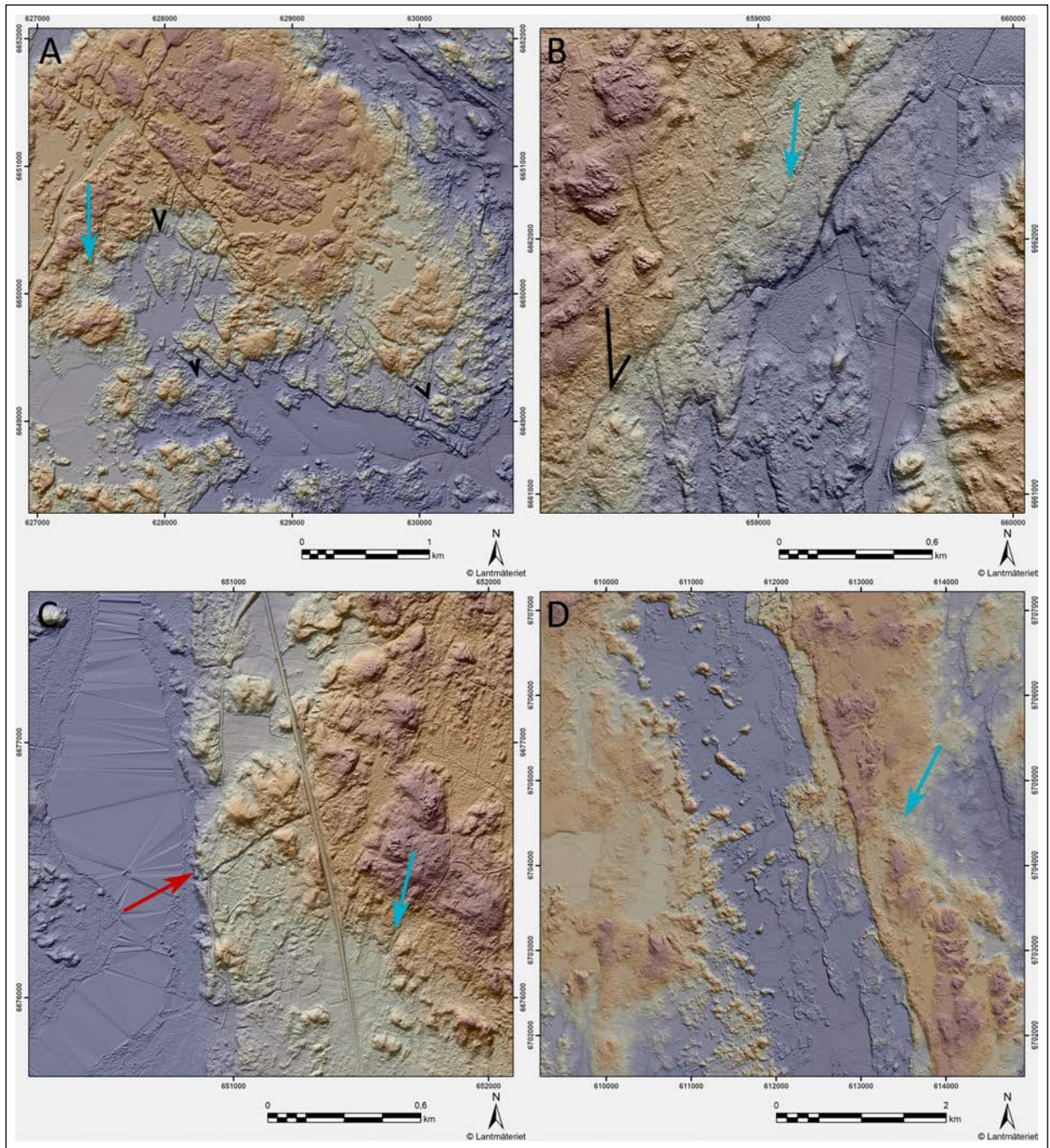


Figure 3-4. Figures of linear features formed by subglacial meltwater. (A) Shows a murtoo tract. (B) Zoomed in view on some murtoo scarps. Black lines are enhancing the visibility of a few V's. Turquoise arrows show ice-flow direction and red arrows highlight scarps. (C) Single murtoo-like scarp. (D) Glaciofluvial corridor (GFC).

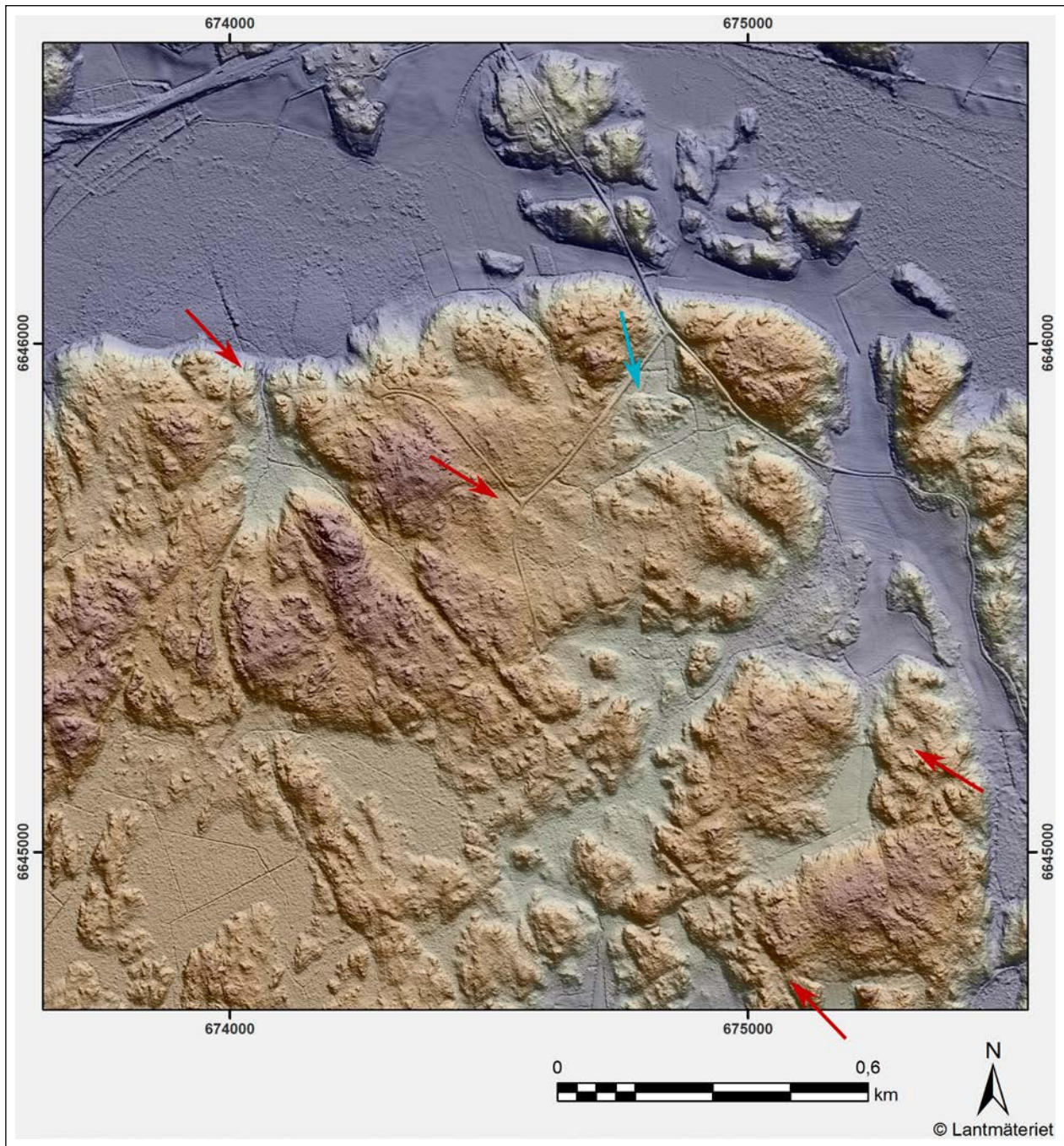


Figure 3-5. Image displays several lineaments. Turquoise arrow show ice-flow direction and red arrows mark lineaments. One in the centre, strikes NW to WNW, is a bit suspicious. No clear and relevant cross-cutting is seen and it is too short. The more obvious lineament is interpreted as an old bedrock structure.

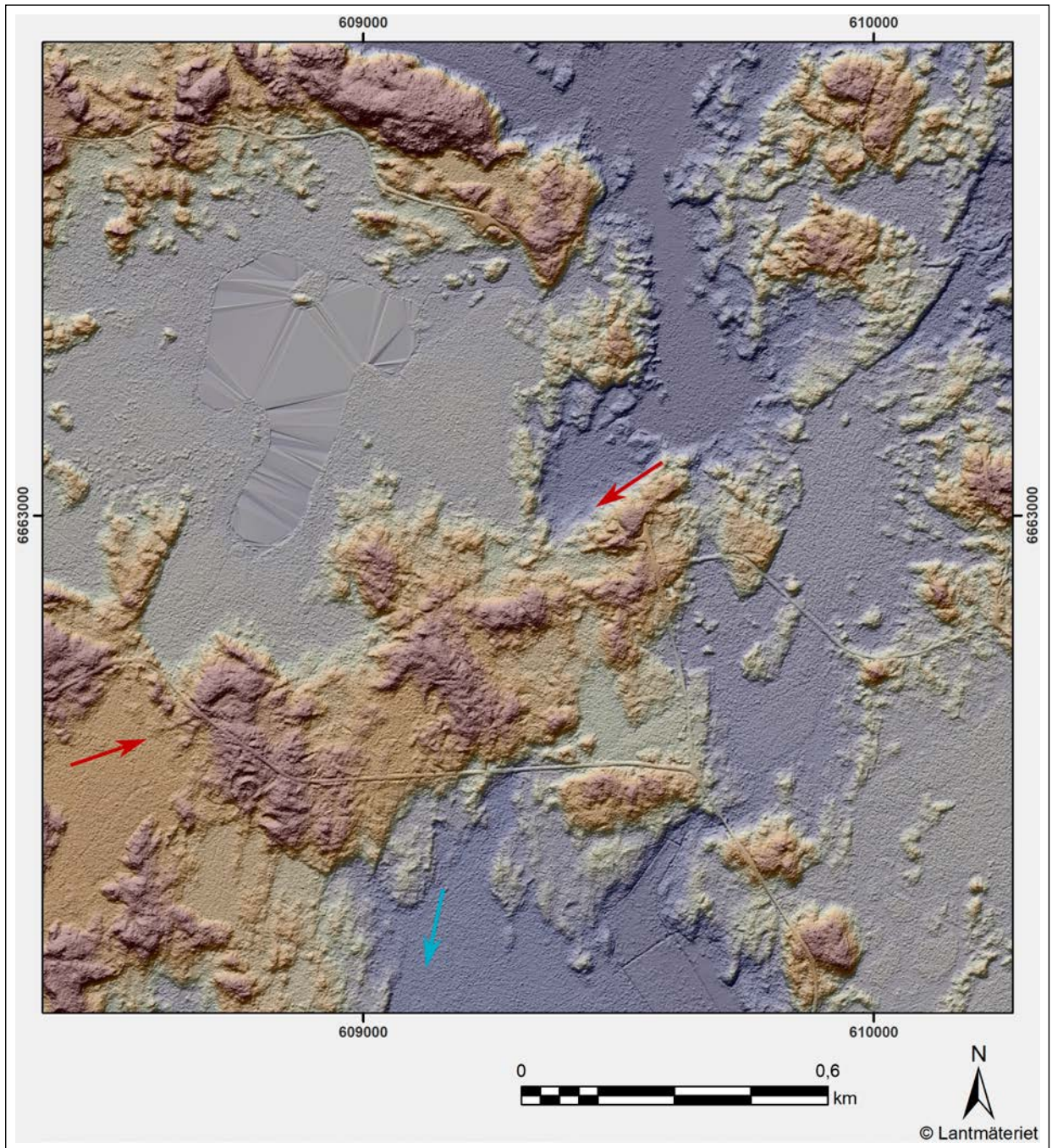


Figure 3-6. A scarp that not clearly cut any Lateglacial-Holocene deposits. It extends into the glaciofluvial scarp in the NE. Turquoise arrow show ice-flow direction and red arrows mark lineaments.

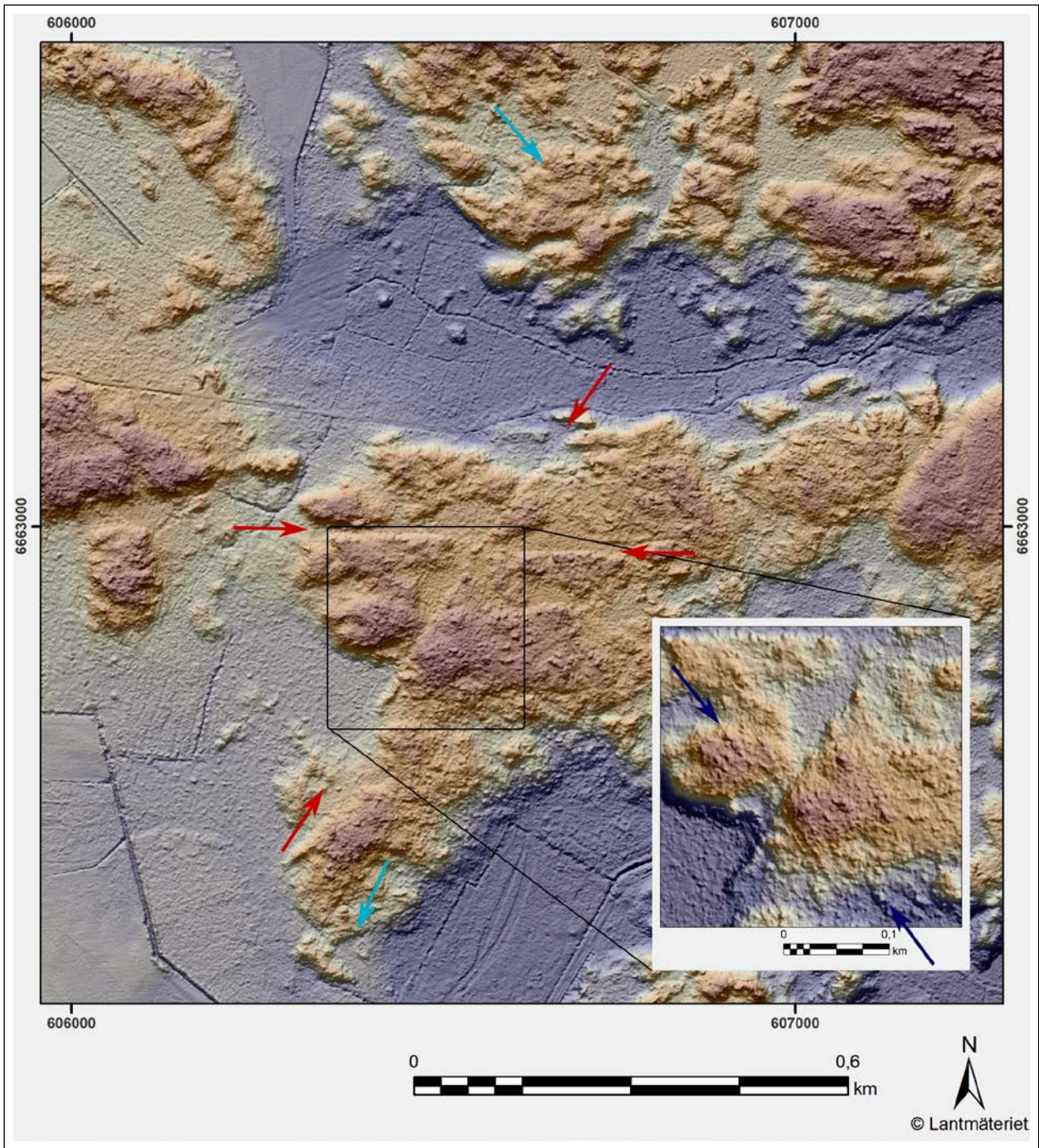


Figure 3-7. Two lineaments cut each other in the centre (red arrows), one W-E and one SSW-NNE. No clear cuts. Two sets of ice-flow direction are detected (Turquoise arrows).

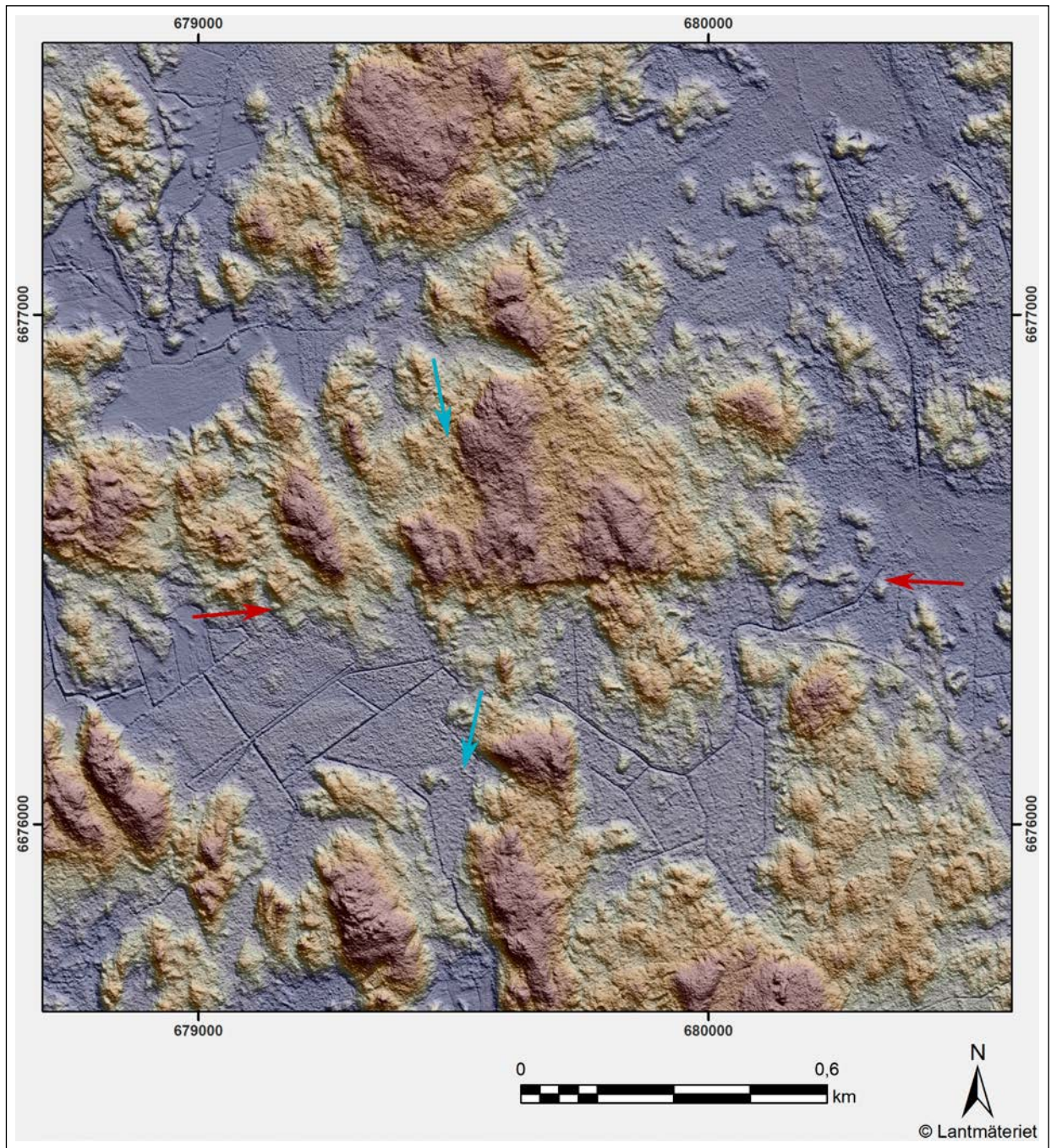


Figure 3-8. Scarp W-E in the center. Does not clearly cut any glacial landforms and it extends into an end moraine to the W. Turquoise arrows show, at least two ice-flow directions and red arrows mark lineaments. The NNE-SSW ice-flow direction is very vague.

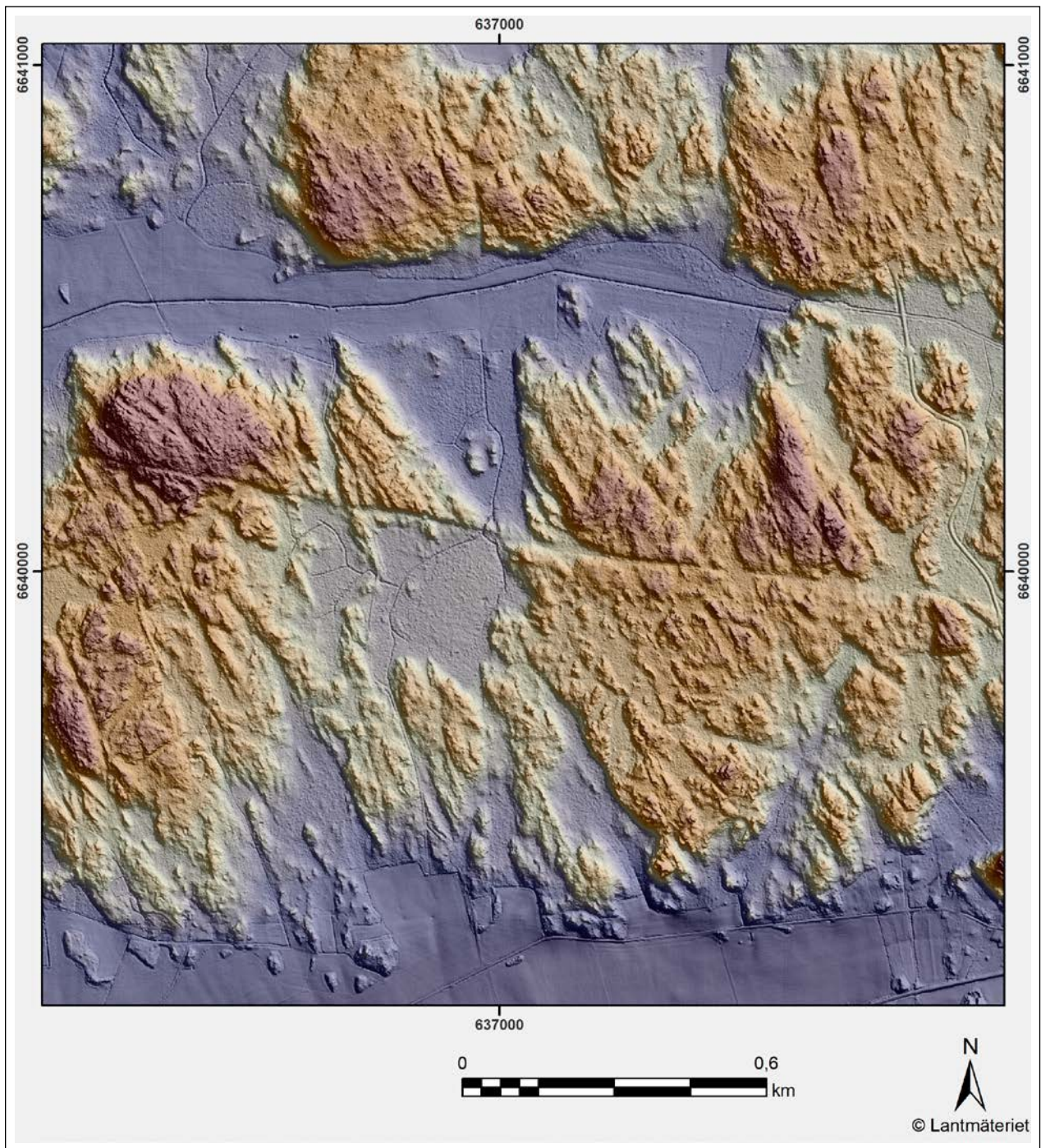


Figure 3-9. Older bedrock structure, not a scarp with an offset – the height is the same on either side. Possibly a weathered hypabyssal rock. Lineaments also in NNW-SSE orientation which appears to be a paleo ice-flow direction from the final retreat of the ice sheet.

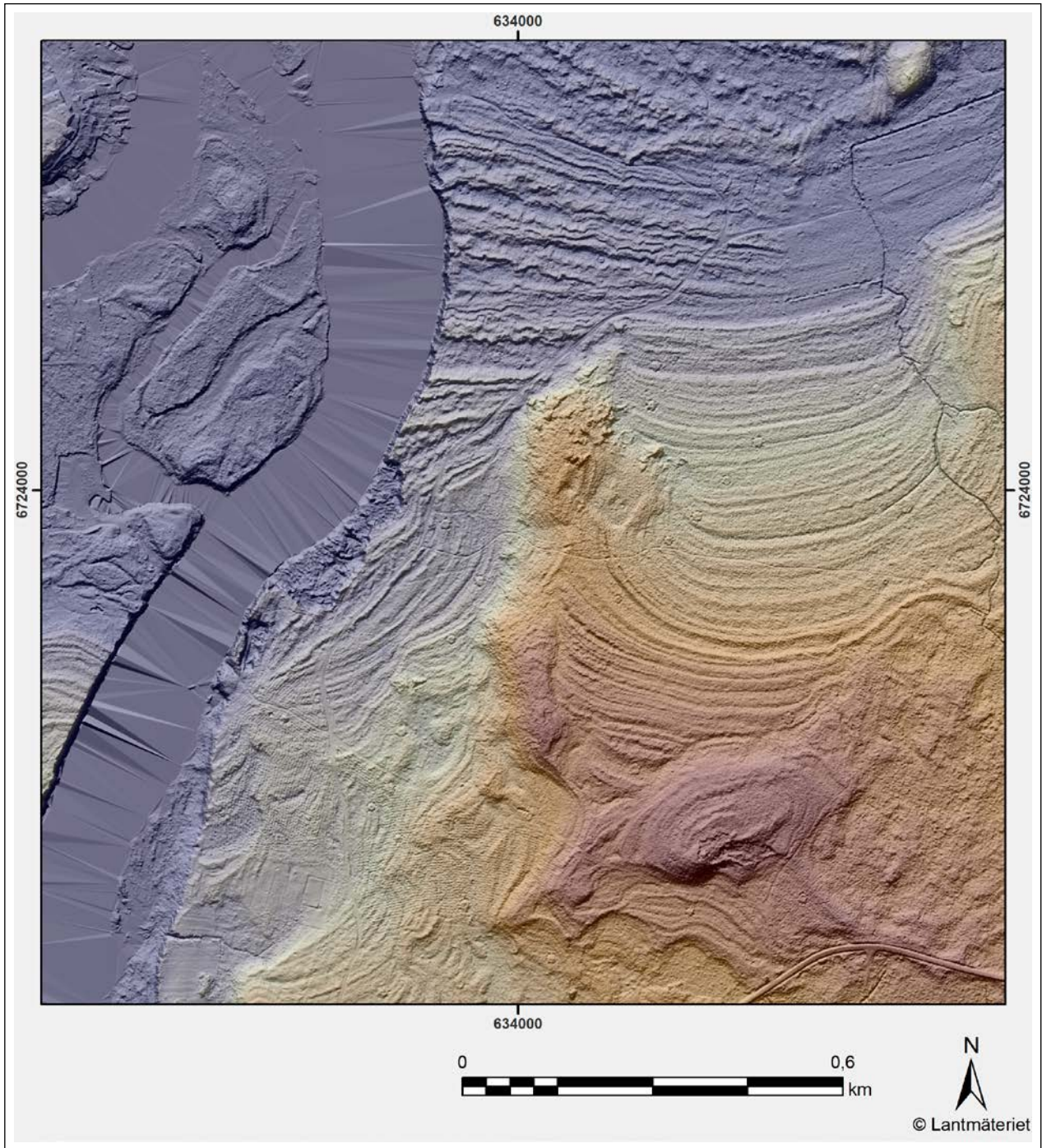


Figure 3-10. Here is an example of two 'scarps' that wrongly could be pointed out in an automated analysis (at least one of them). The SSW-NNE scarp is caused by modern fluvial erosion and the W-E scarps are raised beach ridges.

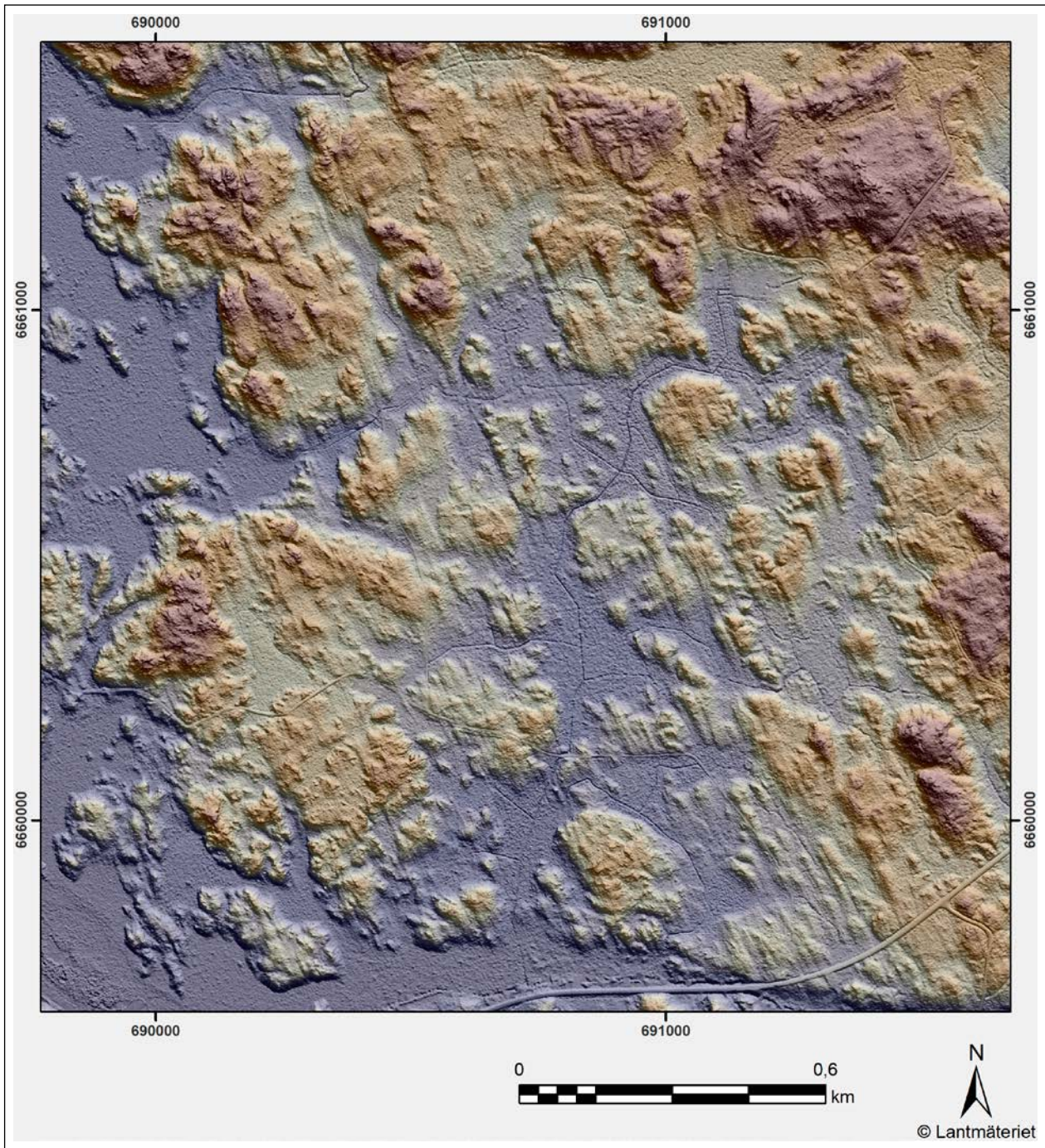


Figure 3-11. A glacially lined landscape. Lineations displays the paleo ice-flow direction. These lineations can occasionally be mistaken for a fault scarp.

4 Discussion

In this study, we have not unambiguously identified any glacially induced fault scarps or landslide scarps. However, the postglacial landscape has been exposed to heavy wave washing that may have erased traces of minor scarps, if they existed. Scarps in glaciofluvial deposits have been used as indicators of a post glacial origin of the fault scarps, as glaciofluvial deposits (i.e. due to their sorted nature) are readily deformed by fault movement (Lagerbäck and Sundh 2008). However, during mapping of surficial deposits in the area it has been shown that glaciofluvial deposits have been considerably remobilized by wave action (Agrell and Mikko 2003), it is common with as much as 10–20 m of postglacial gravel (Sundh and Ericsson 2015). Consequently, if an esker had been crosscut by a fault, the fault's surface expression would most likely have been erased. However, it is still reasonable to assume that fault scarps would be detected as they generally are clearly expressed in the surrounding till covered areas, but without the possibility to decipher their origin by cross-cutting relationships with an esker.

Typical for the screened area is also traces of heavy glaciofluvial erosion that is mainly manifested in several glaciofluvial corridors and abundant sharp scarps related to fluvial actions. These scarps are in places forming fields of murtoos. Some of these scarps have previously been reported, and suggested to be connected to sediment infilling in crevasses at the ice bed interface (Strömberg 1981) or as moraine ridges formed during an extensive ice-sheet readvance (Sandegren 1929, 1948, 1949, Sandegren and Asklund 1946). Relatively often, murtoo landforms display a step-like landscape, which is displayed in Figure 3-4. These step-like formations, or often just parallel ridges, could be mistaken for fault scarps.

Old bedrock structures are manifested as obvious lineations in the landscape, but do not cut Lateglacial-Holocene deposits. They occasionally occur as gorges – two opposite scarps – which can be a representation of a weathered hypabyssal bedrock.

Although no clear PGF's have been found during this screening there are two identified lineaments that are considered as potential PGF's. This is based on crosscutting relations with De Geer moraine ridges and the relative constant offset along the scarp (Figure 3-1). These scarps could very well be murtoo features or older linear-bedrock structures, but we cannot be sure without confirmatory field work.

5 Conclusions

The LiDAR elevation data is stunning in terms of exploring the landscape morphology. The enhanced (1 m cell resolution) data in this study allow us, in places, to detect features not seen in the standard national height model. The entire study area is situated below the highest coastline, thus have been exposed to postglacial sedimentation and erosion. This study intended to reveal and interpret scarps of several types in the search for PGF's or associated landslide scarps. Several interesting scarps have been in question for interpretations. The final focus was only on scarps that seems to cut glacial structures, these are presented in Figure 3-2 and 3-3. In section 6 we suggest a field campaign to assess whether or not the two identified scarps are of a glacial faulting origin or not.

In short, we conclude our work thus:

- Multiple derivatives of a 1m resolution LiDAR DEM was used to screen a 13 225 km² area around the Forsmark area for evidence of potential postglacial seismicity.
- No landforms clearly indicative of postglacial seismicity (i.e. glacial landforms displaced by faults) was discovered during this screening.
- We essentially confirmed previous assessments (e.g. Lagerbäck et al. 2005; Lagerbäck and Sundh 2008).
- We identified two scarps (Figures 3-2 and 3-3) that could represent expressions of paleoseismic activity – crosscutting relations with De Geer moraines – and therefore recommend field investigations.

6 Suggested field-campaign program

To assess whether or not the two identified scarps are of a glacial faulting origin or not, these scarps need to be examined in field.

We propose a campaign composed of a field-reconnaissance part to evaluate the scarps by visual inspection and to identify suitable sites for trenching. Further, we suggest digging along trenches, c. 10 m long at the two selected sites (Figure 3-2 and 3-3), to confirm or refute the faulting origin of these structures.

In the trench cuts, we recommend detailed till-stratigraphy surveys with focus on textures, lithostratigraphy, structures, chemistry and clast fabric.

However, we suspect that geophysical methods also could be required . This would include seismic profiles and/or ground penetrating radar in locations selected during field reconnaissance and after due analysis of the till stratigraphy.

7 Supplementary material

Raster data (TIFF) DEM with a spatial resolution of 1 meter. This was used to generate the different functions that were used for the analyses, saved as a layer file.

An ESRI shape file (polygon feature) presenting the area coverage.

An ESRI shape file (polyline feature) with location and comments on the chosen lineaments for this report.

References

SKB's (Svensk Kärnbränslehantering AB) publications can be found at www.skb.com/publications

Agrell H, Mikko H, 2003. Beskrivning till jordartskartan 12H Söderfors SV. Uppsala Ö Sveriges geologiska undersökning. (Serie Ae 154). (In Swedish.)

Berglund M, Dahlström N, 2015. Postglacial fault scarps in Jämtland, central Sweden. *GFF*, 137, 339–343.

ESRI, 2018. ArcGIS. Redlands, CA: Environmental Systems Resource Institute.

Fenton C H, 1999. Glacio-isostatic (postglacial) faulting: criteria for recognition. In Hanson K L, Kelson K I, Angell M A, Lettis W R (eds). Identifying faults and determining their origins. NUREG/CR-5503, U.S. Nuclear Regulatory Commission, Office of Nuclear Regulatory Research, Appendix A, A-51–A-99.

Hedenström A, Risberg J, 2003. Shore displacement in northern Uppland during the last 6500 calendar years. SKB TR-03-17, Svensk Kärnbränslehantering AB.

Hedenström A, Sohlenius G, Strömberg M, Brydsten L, Nyman H, 2008. Depth and stratigraphy of regolith at Forsmark. Site descriptive modelling SDM-Site Forsmark. SKB R-08-07, Svensk Kärnbränslehantering AB.

Hedin A, 1997. Spent nuclear fuel-how dangerous is it? A report from the project "Description of risk". SKB TR 97-13, Svensk Kärnbränslehantering AB.

Heidbach O, Rajabi M, Reiter K, Ziegler M, WSM Team, 2016. World Stress Map Database Release 2016. GFZ Data Services. Available at: <http://dataservices.gfz-potsdam.de/wsm/showshort.php?id=escidoc:1680890>

Hughes A L C, Gyllencreutz R, Lohne Ø S, Mangerud J, Svendsen J I, 2016. The last Eurasian ice sheets - a chronological database and time-slice reconstruction, DATED-1. *Boreas* 45, 1–45.

Jasiewicz J, Stepinski T F, 2013. Geomorphons – a pattern recognition approach to classification and mapping of landforms. *Geomorphology* 182, 147–156.

Johnson M D, Fredin O, Ojala A E K, Peterson G, 2015. Unraveling Scandinavian geomorphology: the LiDAR revolution. *GFF* 137, 245–251.

Johnson M D, Mäkinen J, Peterson G, Ojala A E K, Palmu J-P, Kajuutti K, Öhrling C, Ahokangas E, 2018. Geomorphology and distribution of subglacial triangular hummocks (murtoos) in Sweden and Finland. In the 33rd Nordic Geological Winter Meeting, Copenhagen, 10–12 January 2018. Copenhagen: Geological Society of Denmark.

Lagerbäck R, Henkel H, 1977. Studier av neotektonisk aktivitet i mellersta och norra Sverige, flygbilds-genomgång och geofysisk tolkning av recenta förkastningar. KBS TR 19, Svensk Kärnbränslehantering AB.

Lagerbäck R, Sundh M, 2008. Early holocene faulting and paleoseismicity in northern Sweden. Uppsala: Sveriges geologiska undersökning. (Research paper C 836). Available at: <http://resource.sgu.se/produkter/c/c836-rapport.pdf>

Lagerbäck R, Sundh M, Svedlund J-O, Johansson H, 2005. Forsmark site investigation. Searching for evidence of late-or postglacial faulting in the Forsmark region. SKB R-05-51, Svensk Kärnbränslehantering AB.

Lidmar-Bergström K, 1982. Pre-Quaternary geomorphological evolution in southern Fennoscandia. Uppsala: Sveriges geologiska undersökning. (Serie C 785)

Lund B, Näslund J-O, 2009. Glacial isostatic adjustment: implications for glacially induced faulting and nuclear waste repositories. In Connor C B, Chapman N A, Connor L J (eds). Volcanic and tectonic hazard assessment for nuclear facilities. Cambridge: Cambridge University Press, 142–155.

Lund B, Schmidt P, Hieronymus C, 2009. Stress evolution and fault stability during the Weichselian glacial cycle. SKB TR-09-15, Svensk Kärnbränslehantering AB.

- Lundqvist J, 2000.** Palaeoseismicity and De Geer Moraines. *Quaternary International* 68, 175–186.
- Lundqvist J, 2010.** Deposits from landslides and avalanches triggered by seismic activity in Swedish Lapland. *Geografiska Annaler, Series A: Physical Geography* 92, 411–420.
- Lundqvist J, Lagerbäck R, 1976.** The parve fault: a late-glacial fault in the Precambrian of Swedish Lapland. *Geologiska Föreningen i Stockholm Förhandlingar* 98, 45–51.
- Martin C D, 2007.** Quantifying in situ stress magnitudes and orientations for Forsmark. Forsmark stage 2.2. SKB R-07-26, Svensk Kärnbränslehantering AB.
- Mikko H, Smith C A, Lund B, Ask M V S, Munier R, 2014.** Neotectonic faulting in Sweden: surface expression from a LiDAR based digital elevation model. In the 31st Nordic Geological Winter Meeting, Lund, Sweden, 8–10 January 2014. Available at: https://www.researchgate.net/profile/Henrik_Mikko/publication/283320846_Neotectonic_faulting_in_Sweden_Surface_expressions_from_the_LiDAR_based_digital_elevation_model/links/5637286908ae758841151f0d/Neotectonic-faulting-in-Sweden-Surface-expressions-from-
- Mikko H, Smith C A, Lund B, Ask M V S, Munier R, 2015.** LiDAR-derived inventory of post-glacial fault scarps in Sweden. *GFF* 137, 334–338.
- Muir-Wood R, 2000.** Deglaciation seismotectonics: a principal influence on intraplate seismogenesis at high latitudes. *Quaternary Science Reviews* 19, 1399–1411.
- Mörner N-A, 2005.** An interpretation and catalogue of paleoseismicity in Sweden. *Tectonophysics* 408, 265–307.
- Palmu J-P, Ojala A E K, Ruskeeniemi T, Sutinen R, Mattila J, 2015.** LiDAR DEM detection and classification of postglacial faults and seismically-induced landforms in Finland: a paleoseismic database. *GFF* 137, 344–352.
- Persson C, 1988.** Beskrivning till Jordartskartan Östhammar SO. Uppsala: Sveriges geologiska undersökning. (Serie Ae 90). (In Swedish.)
- Peterson G, Johnson M D, 2018.** Hummock corridors in the south-central sector of the Fennoscandian ice sheet, morphometry and pattern. *Earth Surface Processes and Landforms* 43, 919–929.
- Påsse T, Daniels J, 2015.** Past shore-level and sea-level displacements. Uppsala: Sveriges geologiska undersökning. (Rapporter och meddelanden 137)
- Sandegren R, 1929.** Om isrecessionen i Gefletrakten och den senkvartära geokronologien. *Geologiska Föreningen i Stockholm Förhandlingar* 51, 573–579. (In Swedish.)
- Sandegren R, 1948.** Jordlagren. Beskrivning till kartbladet Söderfors. Stockholm: Sveriges geologiska undersökning. (Serie Aa 190). (In Swedish.)
- Sandegren R, 1949.** Jordlagren. Beskrivning till kartbladet Untra. Stockholm: Sveriges geologiska undersökning. (Serie Aa 191). (In Swedish.)
- Sandegren R, Asklund B, 1946.** Beskrivning till kartbladet Möklinta. Stockholm: Sveriges geologiska undersökning. (Serie Aa 186). (In Swedish.)
- SGU, 2015a.** Produkt: Jorddjupsmodell (Drift-Depth model, 10x10 m). Uppsala: Sveriges geologiska undersökning. Available at: <http://resource.sgu.se/dokument/produkter/jorddjupsmodell-beskrivning.pdf> (In Swedish.)
- SGU, 2015b.** Produkt: Högsta kustlinjen (Highest coastline). Uppsala: Sveriges geologiska undersökning. Available at: <http://resource.sgu.se/dokument/produkter/hogsta-kustlinjen-beskrivning.pdf> (In Swedish.)
- SGU, 2016.** Produkt: Jordskred och raviner (Landslides and gullies). Uppsala: Sveriges geologiska undersökning. Available at: <http://resource.sgu.se/dokument/produkter/jordskred-raviner-beskrivning.pdf> (In Swedish.)
- SKB, 2011.** Long-term safety for the final repository for spent nuclear fuel at Forsmark. Main report of the SR-Site project. Volume II. SKB TR-11-01, Svensk Kärnbränslehantering AB.

- Smith C A, Sundh M, Mikko H, 2014.** Surficial geology indicates early Holocene faulting and seismicity, central Sweden. *International Journal of Earth Sciences* 103, 1711–1724.
- Sohlenius G, Hedenström A, Rudmark L, 2004.** Forsmark site investigation. Mapping of unconsolidated Quaternary deposits 2002–2003. Map description. SKB R-04-39, Svensk Kärnbränslehantering AB.
- Stephens M B, Bergman T, Isaksson H, Petersson J, 2008.** Bedrock geology Forsmark. Modelling satge 2.3. Description of the bedrock geological map at the ground surface. SKB R-08-128, Svensk Kärnbränslehantering AB.
- Stroeven A P, Hättestränd C, Kleman J, Heyman J, Fabel D, Fredin O, Goodfellow B W, Harbor J M, Jansen J D, Olsen L, Caffee M W, Fink D, Lundqvist J, Rosqvist G C, Strömberg B, Jansson K N, 2016.** Deglaciation of Fennoscandia. *Quaternary Science Reviews*, 147, 91–121.
- Strömberg B, 1981.** Calving bays , striae and moraines at Gysinge-Hedesunda, central Sweden. *Geografiska Annaler* 63, 149–154.
- Sundh M, Ericsson B, 2015.** Beskrivning till jordartskartorna 13H Gävle NV, NO, SV och SO. Uppsala: Sveriges geologiska undersökning. (Serie K 513–516). (In Swedish.)
- Söderbäck B (ed), 2008.** Geological evolution, palaeoclimate and historical development of the Forsmark and Laxemare-Simpevarp area. Site descriptive modelling, SDM-Site. SKB R-08-19, Svensk Kärnbränslehantering AB.
- Utting D J, Ward B C, Little E C, 2009.** Genesis of hummocks in glaciofluvial corridors near the Keewatin Ice Divide, Canada. *Boreas* 38, 471–481.
- Wilson M F J, O’Connell B, Brown C, Guinan J C, Grehan A J, 2007.** Multiscale terrain analysis of multibeam bathymetry data for habitat mapping on the continental slope. *Marine Geodesy* 30, 3–35.

SKB is responsible for managing spent nuclear fuel and radioactive waste produced by the Swedish nuclear power plants such that man and the environment are protected in the near and distant future.

skb.se